Atmospheric Environment 138 (2016) 114–124

Contents lists available at ScienceDirect

Atmospheric Environment

journal homepage: www.elsevier.com/locate/atmosenv

Individual particles of cryoconite deposited on the mountain glaciers of the Tibetan Plateau: Insights into chemical composition and sources

Zhiwen Dong [a, *], Dahe Qin [a], Shichang Kang [a, b], Yajun Liu [a], Yang Li [c], Jie Huang [c], Xiang Qin [a]

[a] State Key Laboratory of Cryospheric Sciences, Cold and Arid Regions Environmental and Engineering Research Institute, Chinese Academy of Sciences, Lanzhou 730000, China
[b] CAS Center for Excellence in Tibetan Plateau Earth Sciences, Beijing 100101, China
[c] Institute of Tibetan Plateau Research, Chinese Academy of Sciences, Beijing 100101, China

HIGHLIGHTS

- We present morphology and chemical composition of cryoconite in the Tibetan Plateau.
- Mineral dust particles was dominant (>50%) in the cryoconite at all locations.
- More BC and fly ash particles were found in YL (38%) and ZD (22%).
- A large amount of biological, NaCl and MCS particles were observed.

ARTICLE INFO

Article history:
Received 12 January 2016
Received in revised form
9 May 2016
Accepted 9 May 2016
Available online 10 May 2016

Keywords:
Cryoconite
TEM-EDX
Light absorbing impurities
Tibetan Plateau

ABSTRACT

Cryoconite deposited on mountain glacier surfaces is significant for understanding regional atmospheric environments, which could influence the albedo and energy balance of the glacier basins, and maintain the glacial microbiology system. Field observations were conducted on the glaciers of western China, including Laohugou Glacier No.12 (LHG), Tanggula Dongkemadi Glacier (TGL), Zhadang Glacier (ZD), and Baishui Glacier No.1 in the Yulong Mountains (YL), as well as Urumqi Glacier No.1 in the Tianshan Mountains (TS) for comparison with locations in the Tibetan Plateau, in addition to laboratory TEM-EDX analysis of the individual cryoconite particles filtered on lacey carbon (LC) and calcium-coated carbon (Ca-C) TEM grids. This work provided information on the morphology and chemical composition, as well as a unique record of the particle's physical state, of cryoconite deposition on the Tibetan Plateau. The result showed that there is a large difference in the cryoconite particle composition between various locations on the Tibetan Plateau. In total, mineral dust particles were dominant (>50%) in the cryoconite at all locations. However, more anthropogenic particles (e.g., black carbon (BC) and fly ash) were found in YL (38%) and ZD (22%) in the Ca-C grids in the southern locations. In TGL, many NaCl and MCS particles (>10%), as well as few BC and biological particles (<5%), were found in cryoconite in addition to mineral dust. In TS, the cryoconite is composed primarily of mineral dust, as well as BC (<5%). Compared with other sites, the LHG cryoconite shows a more complex composition of atmospheric deposition with sufficient NaCl, BC, fly ash and biological particles (6% in LC grid). The higher ratio of anthropogenic particles in the southern Tibetan Plateau is likely caused by atmospheric pollutant transport from the south Asia to the Tibetan Plateau. Cryoconite in the northern locations (e.g., TGL, LHG, and TS) with higher dust and salt particle ratio are influenced by large deserts in central Asia. Therefore, the transport and deposition of cryoconite is of great significance for understanding regional atmospheric environment and circulation. Large amounts of biological, NaCl and MCS particles were observed in the cryoconite, implying that in addition to dust and BC, many types of light absorbing impurities (LAI) together could influence the glacier albedo change and induce ice melting in the mountain glaciers of the Tibetan Plateau. Moreover, a high BC concentration in the south (e.g., YL and ZD) could significantly change the albedo

* Corresponding author.
E-mail address: dongzhiwen@lzb.ac.cn (Z. Dong).

http://dx.doi.org/10.1016/j.atmosenv.2016.05.020

of snow and ice, at a greater rate than dust, causing significant melting of the glaciers under global warming.

1. Introduction

Cryoconite deposited on the mountain glacier surfaces is significant for understanding regional atmospheric environments, which could influence the albedo and energy balance of the glacier regions and maintain the glacial microbiology system. Research has indicated that cryoconite originates from the atmospheric deposition of various light absorbing impurities (LAI) in the snowpack and ice surfaces on high mountains (Stibal et al., 2012). With increased glacier ablation, the impurities melted and subsequently accumulated on the glacier surface (Wharton et al., 1985). Cryoconite has a dark color and generally consists of mineral dust, black carbon (BC) and biological particles (Takeuchi and Li, 2008; Grzesiak et al., 2015), which reduces the energy balance of the glaciers and accelerates glacier melting (Fujita, 2002; Oerlemans et al., 2009; Wientjes et al., 2011; Naegeli et al., 2015). Each component of LAI has different radiative forcing in the atmosphere and cryoconite (IPCC AR5). Therefore, studying the cryoconite deposition under recent dramatic glacier change when water resources might be impacted is important.

Previous studies have characterized the biological composition of cryoconite and its climate effects in the Arctic and Asian regions (e.g. Takeuchi et al., 2001, 2003; Margesin et al., 2002; Anesio et al., 2009; Singh et al., 2015; Grzesiak et al., 2015). In addition, some studies have provided the mineralogical and geochemical information for cryoconite in central Asia (Nagatsuka et al., 2014), and biological processes that occur on the surface cryoconite of glaciers and ice sheets can affect the physical behavior of glaciers by changing surface reflectivity (Stibal et al., 2012). Moreover, transmission electron microscope (TEM) is a good method to learn the particle morphology and physicochemical composition (Semeniuk et al., 2014). For example, study based on observation and TEM analysis has found that dust and biological aerosols from the Sahara and Asia may influence precipitation in the Western U.S. (Creamean et al., 2013). However, few studies have been conducted on the morphology, chemical composition and the particle's physical state of cryoconite deposition on the alpine glaciers in the Tibetan Plateau and central Asia.

The Tibetan Plateau is called as "The Third Pole" of the earth, with a large number of glaciers existing in the high mountains. However, limited study of cryoconite on the glaciers in the Tibetan Plateau has been conducted, due to its high altitude and remote location. As a result, information on the physiochemical composition and sources of cryoconite is still lacking; e.g., BC, dust, and biological particles deposited on the glacier surface over the different locations of the Tibetan Plateau, which could provide regional atmospheric environment information at a large scale, as well as its transport route with atmospheric circulation. Therefore, field observations were conducted on the glaciers of western China, including Laohugou Glacier No.12 (LHG), Tanggula Dongkemadi Glacier (TGL), Zhadang Glacier (ZD), and Baishui Glacier No.1 in the Yulong Mountains (YL), as well as Urumqi Glacier No.1 in the Tianshan Mountains (TS) for comparison with locations in the Tibetan Plateau, in addition to laboratory TEM-EDX analysis of the individual cryoconite particles filtered on lacey carbon (LC) and calcium-coated carbon (Ca-C) TEM grids. This work provided information on the morphology and chemical composition, as well as a unique record of the particle's physical state of cryoconite deposition on the Tibetan Plateau, to determine its source and transport route under the influence of regional atmospheric circulation.

2. Data and methods

From July to September in 2014, we collected cryoconite samples on the glaciers at five different locations in the Tibetan Plateau, including Laohugou Glacier No.12 (LHG), Tanggula Dongkemadi Glacier (TGL), Zhadang Glacier (ZD), and Baishui Glacier No.1 in the Yulong Mountains (YL), as well as Urumqi Glacier No.1 (43°05′N, 86°48′E) in the Tianshan Mountains (TS) for comparison with locations in the Tibetan Plateau (Fig. 1). Among these glaciers, the LHG Glacier No.12 (39°20′N, 96°34′E) and HLG Shiyi Glacier (33°13′N, 99°53′E) are located in the northeast Tibetan Plateau on the northern slope of the Qilian Mountains with typical continental climatic conditions (Dong et al., 2014). Dongkemadi Glacier (33°04′N, 92°04′E) is located in the Tanggula Mountains of the central Tibetan Plateau. While Zhadang Glacier (30°28′N, 90°38′E) is located on the western Nyainqentanglha in the southern Tibetan Plateau, and Baishui Glacier No.1 (27°18′N, 100°08′E) in the Yulong Mountains is located in the southeast Tibetan Plateau, with typical Monsoon climatic conditions (Fig. 1). Therefore, these locations could represent the large scale deposition of cryoconite on the glaciers in the Tibetan Plateau. The information on sampling location, time period and snow depth are shown in Table 1. Cryoconite samples were collected at different elevations along the glacier surface of the study. Pre-cleaned low-density polyethylene (LDPE) bottles (Thermo scientific) were used for the sample collection. All samples were kept frozen until they were transported to the lab for analysis.

Analyses of the individual cryoconite particles were conducted using a JEM-2100F (JEOL) transmission electron microscope (TEM) operated at 200 kV. The analyses involved conventional and high-resolution imaging using bright field mode, electron diffraction (Zinatloo-Ajabshir et al., 2015, 2016; Salavati-Niasari, 2005), and energy-dispersive X-ray spectrometry (EDX). A qualitative survey of grids was undertaken to assess the size and compositional range of particles and to select areas for more detailed quantitative work that were representative of the entire sample. This selection ensured that despite the small percentage of particles analyzed quantitatively, our results were consistent with the qualitative survey of the larger particle population on each grid. Quantitative information on size, shape, composition, speciation, mixing state, and physical state was collected for a limited set of stable particles. Volatile particles, including nitrate, nitrite, and ammonium sulfate, are not stable under the electron beam and could not be measured accurately in this study, although they can often be detected on EDX at low beam intensity. All stable particles with sizes 20 nm to 35 μm were analyzed within representative grid mesh squares located near the center of the grid. Grid squares with moderate particle loadings were selected for study to preclude the possibility of overlap or aggregation of particles on the grid after sampling. In general, 100 particles were analyzed per grid, yielding totals of ~300 particles per sample (from the three grid fractions). The use of LC and Ca-C grids resulted in clear and unprecedented physical and

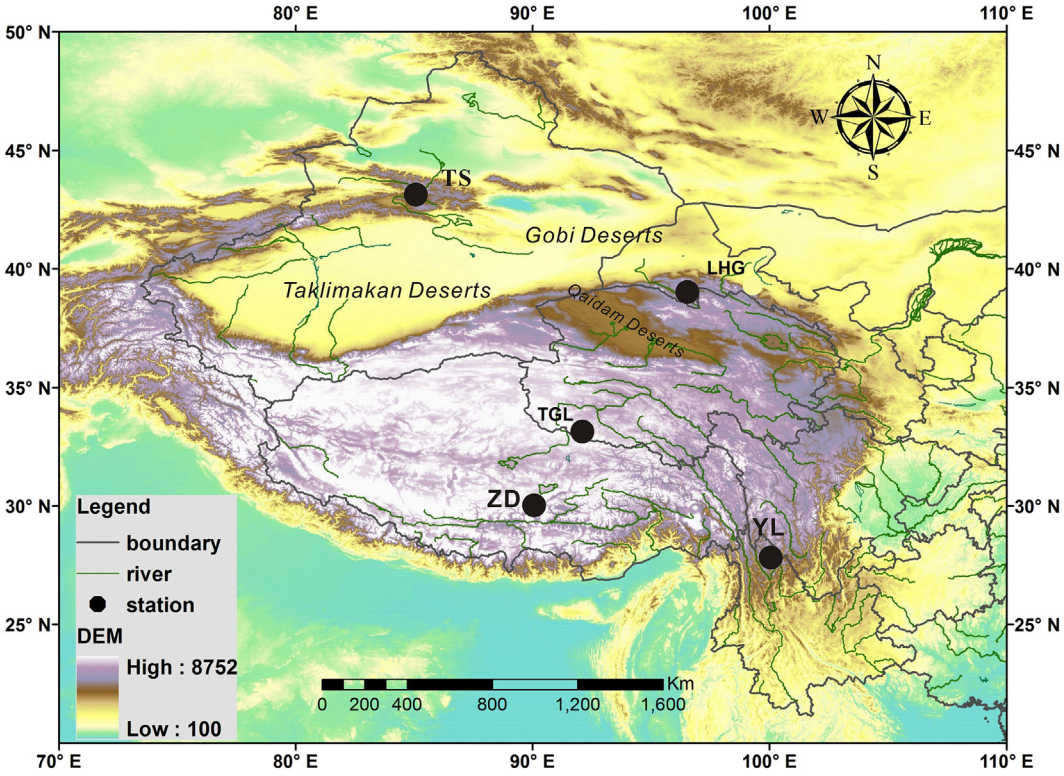

Fig. 1. Map showing the locations of the cryoconite sampling glaciers in western China, including Laohugou GlacierNo.12 (LHG), Tanggula Dongkemadi Glacier (TGL), Zhadang Glacier (ZD), and Baishui Glacier No.1 in the Yulong Mountains (YL), as well as Urumqi Glacier No.1 in the Tianshan Mountains (TS).

Table 1
Information on sampling location, altitude, time and snow depth for TEM-EDX analysis.

Sample	Locations	Altitude (m a.s.l.)	Date	Snow depth (cm)
LHG29-1	LHG	4590	2014-7-29	5
LHG29-3	LHG	4386	2014-7-29	5
LHG30-4	LHG	4698	2014-7-30	5
LHG8-4	LHG	4850	2014-8-8	5
TGL18-9	TGL	5464	2014-8-19	5
TGL18-10	TGL	5466	2014-8-19	5
TGL18-18	TGL	5604	2014-8-19	5
TGL18-19	TGL	5603	2014-8-19	5
TS-31-5	TS	3871	2014-8-31	5
TS-31-9	TS	3798	2014-8-31	5
TS-1-2	TS	3939	2014-9-1	5
TS-1-4	TS	4000	2014-9-1	5
YL-17-5	YL	4750	2014-8-17	5
YL-17-1	YL	4775	2014-8-17	5
YL-19-4	YL	4636	2014-8-19	5
YL-19-2	YL	4601	2014-8-19	5
ZD-1	ZD	5579	2014-9-13	5
ZD-2	ZD	5639	2014-9-13	5
ZD-3	ZD	5727	2014-9-13	5
ZD-4	ZD	5605	2014-9-13	5

chemical information for the individual particle types.

3. Results and discussion

3.1. Morphology, chemical composition and particle's physical state of cryoconite

Using TEM analysis, we easily observed the morphology of various components of the cryoconite in the samples, and, combined with EDX analysis, we obtained the chemical composition and mineralogy of individual particles. The "transmission" feature of TEM also makes the analysis possible to obtain the "inside" morphology of the cryoconite particles. As shown in Fig. 2, we obtained the bright image of individual cryoconite particles with different physical state in the samples on the LC grids at the LHG Glacier. During the analysis, we should firstly find out the different particles of natural and anthropogenic sources through the morphology and EDX analysis (Fig. 2). Generally, mineral dust particles often show the irregular shape and sharp margin that originates from the earth's crustal surface and long range transport in the atmosphere, which often contain significant Si-, Al-, Ca-, K-, and Fe-rich materials (Dong et al., 2014, 2015). For example, in Fig. 2g, the quartz particle exhibited a chemical composition of SiO_2 and attached Al-, Na-rich materials on the surface in the cryoconite (Fig. 2g and h). However, we also observed many individual particles with a morphology that was cotton-shaped and black in color, which appears to originate from burning soot (Fig. 2a). Combined with the chemistry analysis, we determined these particles were mainly composed of a Carbon-element, and thus were defined as black carbon (BC) particles. Such BC particles were observed in a large amount (high ratio) in the glacier cryoconite at five different locations in this study. The particles with similar anthropogenic sources as fusel materials burning with high temperature were fly ash and soot particles. In addition to mineral and anthropogenic particles, many particles with a regular shape and smooth edges, such as biological tissue, were present (Fig. 2c, e). The EDX analysis showed that the chemical constitutes were mainly composed of C and O, in addition to other trace elements (see Fig. 2d, f). We defined these particles as biological particles, showing the chemical constitutes of biological tissue, always aggregated with mineral particles (Fig. 2c, e). From the above analysis, we determined that the individual particles of cryoconite were composed primarily of

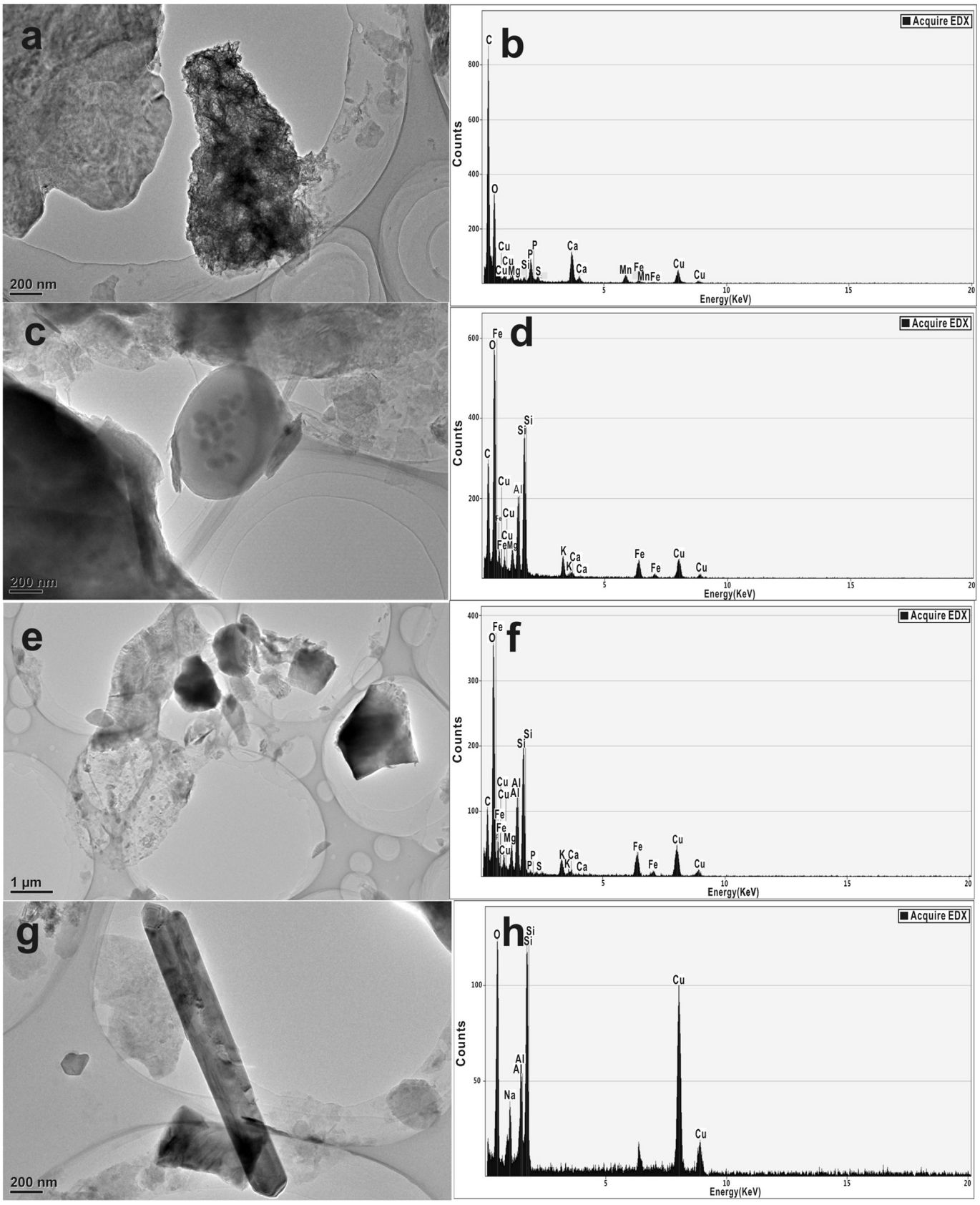

Fig. 2. (a) BC particles; (c) biological/mineral aggregate particles; (e) mineral-biological particles; (g) mineral particles (SiO_2), and EDX analysis of chemical composition (b, d, f, h) for various individual particle types derived from the LHG cryoconite.

mineral particles, BC-fly ash-soot particles and biological particles.

Fig. 3 shows the TEM bright-field images of the typical individual particles from the LC grids for the cryoconite samples at the different locations of the Tibetan Plateau. LC grids have many filtration pores in the surface, which could filter out some finer cryoconite particles and make the large particles clearly visible for observation. In total, the particles were composed frequently of silicate, sulfate minerals (Fig. 3a) and NaCl particles (Fig. 3c, f), in addition to BC, fly ash and soot from anthropogenic sources (Fig. 3b–e). Biological particles were also found in these glaciers of the Tibetan Plateau (Fig. 3f), and in particularly large amounts in the LHG Glacier cryoconite samples (accounting for approximately 6% of the LHG cryoconite). These individual particles composed the total physical state of the cryoconite deposited on the mountains glaciers in the Tibetan Plateau, which often appeared as either individual particles or aggregated particles, as shown in Fig. 3b and f. The physical types of the individual particles and their aggregated style of cryoconite on the LC grids were shown in Table 2, while Table 3 shows the particle types amalgamated for Figs. 2 and 3.

Compared with the LC grid, the Ca-C grid has no filtration pores in the surface, which thus could absorb the majority of the fine-ultrafine particles during filtration. This feature makes the observation easier to determine and study the fine cryoconite particles, particularly for particles with a diameter of 20–500 nm. Therefore, we also used Ca-C grid filter to process the cryoconite samples derived from the mountains glaciers in the Tibetan Plateau for TEM analysis (Fig. 4). We observed a clear difference between the LC grid and Ca-C grid results. A greater number of fine particles were observed on the Ca-C grid, among which a large amount of anthropogenic particles (e.g., BC, fly ash and soot) were observed, more than on the LC grid (Fig. 4a, c, e). Meanwhile, we observed many fine particles of mixed cation sulfate (MCS, see Fig. 4a, d) and NaCl droplet (Fig. 4b), which originated from the atmospheric Light Absorbing Impurities deposition to the glacier surface and may cause the snow and ice albedo to change significantly. In total, these anthropogenic particles generally appeared as aggregated particles. The BC, fly ash, and soot particles generally aggregated together, which may be due to their similar transport route and sources. In addition, BC and fly ash generally found aggregated with mineral dust particles (Fig. 4a and f) in the cryoconite of the different locations, indicating the effect of mineral dust on anthropogenic particles during transport. During long range transport, the dust

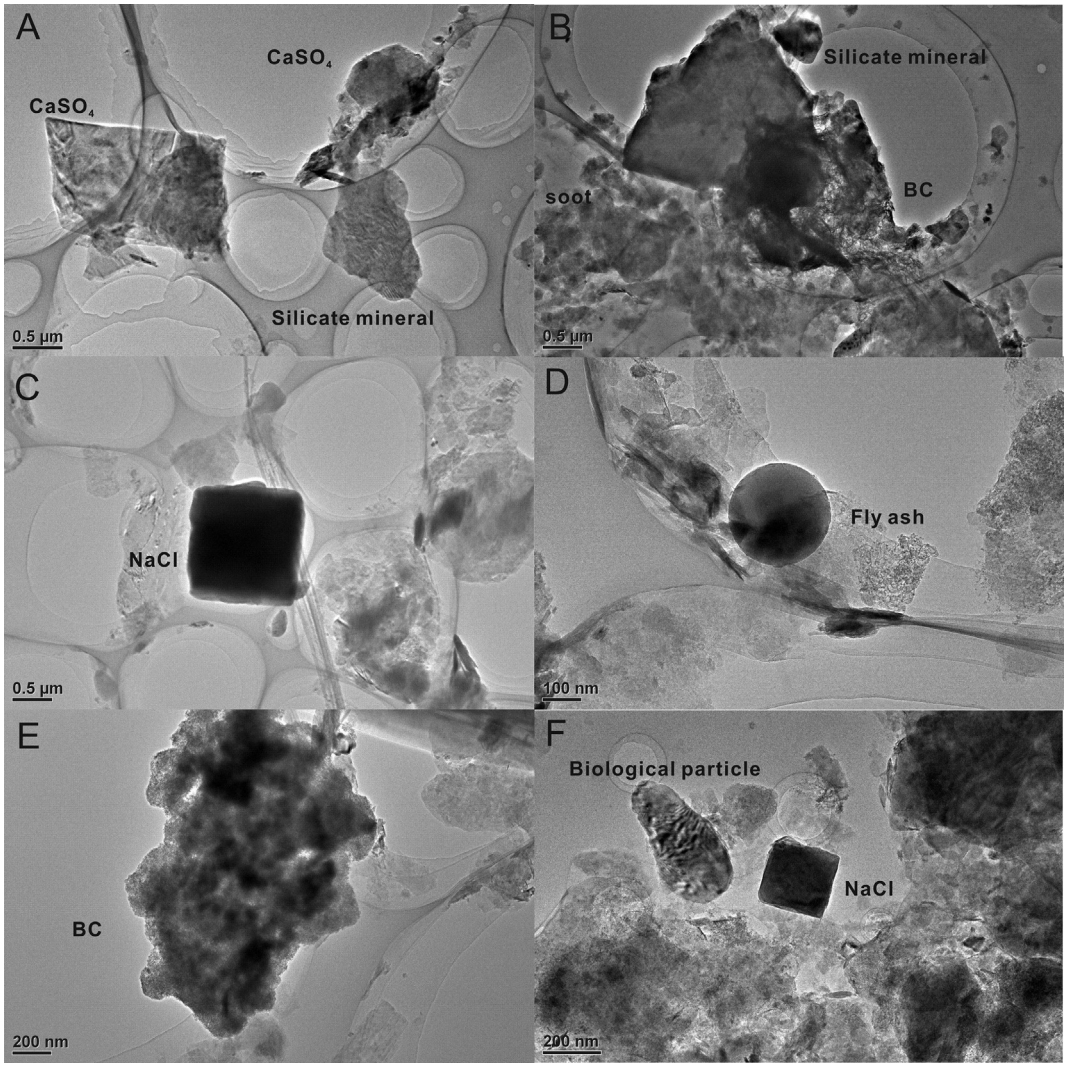

Fig. 3. Bright-field images of typical individual particles from the LC grids: (a) Silicate aggregate particles with additional mixed cation sulfate (MCS) components; (b) BC/Silicate and soot mixed aggregate particles; (c)a NaCl single grain; (d) a fly ash/Silicate aggregate particle; (e) a BC aggregate particle; and (f) a NaCl single grain and biological/Silicate aggregate particle.

Table 2
The individual particles identified on the LC Grids for cryoconite deposited on the glaciers of the Tibetan Plateau.

Particle type	Chemical composition of particles in effloresced state (LC grids)
Single particles	1. Silicate
	2. Carbonate
	3. Salt (NaCl)
	4. Soot (ns)
	5. Organic
	6. Black carbon
	7. Fly ash
	8. sulfate salts
	9. Quartz
	10. Aluminate[a]
	11. Albite
Internally mixed particles	12. Silicate/silicate aggregate
	13. Silicate/carbonate aggregate
	14. Silicate/Fe-oxide aggregate
	15. Silicate/soot (ns) aggregate
	16. Silicate/NaCl aggregate
	17. Silicate/MCS
	18. Soot (ns)/MCS
	19. Carbonate/MCS
	20. Mixed cation sulfate salts (MCS)

[a] Particle type is present at less than 1% frequency.

Table 3
Table showing the particle types amalgamated for Fig. 3.

Categories shown in Fig. 3	Categories amalgamated from Table 2
Mineral grain	1, 2, 8
NaCl single grain	3
Mineral aggregate not containing NaCl	11, 12, 13
Mineral aggregate containing NaCl	16
BC single grain	4, 6
Mineral aggregate containing BC	15
Soot (ns) or Soot (ns)-containing particle	15, 18
Fly ash single grain	7
Mineral aggregate containing Fly ash and soot	15
Organic single grain	5

particle could absorb and transport anthropogenic particles in the free troposphere to the glacier basins in the Tibetan Plateau. When resisted by the high mountains during transport, these atmospheric aggregated particles will deposit on the glacier surface with snow fall to the cryoconite particles together with biological particles. Therefore, based on the LC grid and Ca-C grid of TEM analysis, we easily obtain the components of the cryoconite, and subsequently evaluated its physicochemical composition and source.

Upon finishing the analysis of the composition and physical state of cryoconite, we needed to evaluate the composition ratio of each components (e.g., mineral dust, BC, fly ash and soot, and biological particles), as their radiative forcing is extremely different, e.g. BC showing larger radiative forcing than dust (IPCC AR5). Because of the long range distribution of the sampling locations in this work, the surrounding environment of each location was very different from each other. For example, Urumqi Glacier No.1 (TS) is located in central Tianshan Mountains, and the atmospheric environment of the glacier basin was significantly influenced by both nearby anthropogenic industries emission (e.g., BC) and dust activities in central Asia (Xinjiang province of China). Differently, the glacier basins in Tibetan Plateau are located in more remote areas, with long range distributed and different atmospheric environment between the north and the south of “The Third Pole”.

By analyzing the TEM image, we obtained the relative composition ratio of cryoconite on the LC and Ca-C grids for samples from different locations of the Tibetan Plateau (Fig. 5). Due of the difference in filter grid, a difference in the composition ratio of cryoconite components between the LC grid and Ca-C grid exists. However, the result is still similar for spatial comparison based on the two types of grid, which could reflect the spatial difference for distinct cryoconite deposition (Fig. 5). On the Ca-C grid, the anthropogenic particles (e.g. BC, soot and fly ash) showed an increased composition ratio in cryoconite, which was reflected in all glaciers. In total, mineral dust particles were dominant in the cryoconite deposited in different locations on the Tibetan Plateau (all greater than 50%), while the other compositions (e.g., BC) also exhibited a difference between cryoconite in each glacier area. We observed that more anthropogenic particles (e.g., BC and fly ash) were found in YL (38%) and ZD (22%) in Ca-C grids in the south of the Tibetan Plateau (Fig. 5). In TGL, many NaCl and MCS particles (>10%), as well as BC and biological particles (<5%), were observed in the cryoconite, in addition to mineral dust. In TS, the cryoconite is composed primarily of mineral dust, in addition to BC (<5%). Compared with other sites, the LHG cryoconite exhibited a more complex composition of atmospheric deposition (Fig. 5), with sufficient NaCl, BC, fly ash and biological particles (6% in LC grid). The higher ratio of anthropogenic particles in the southern Tibetan Plateau is likely caused by atmospheric pollutant transport from southern Asia to the Tibetan Plateau. Cryoconite in the northern locations (e.g., TGL, LHG, and TS) with a higher dust and salt particle ratio are likely influenced by large deserts in central Asia. Furthermore, a large amount of biological particles and NaCl and MCS salt particles were observed, implying that the cryoconite was composed of complex constitutes acting as light absorbing impurities, which together could impact the radiative forcing on the glacier and thus cause accelerated glacier melting. Moreover, a high

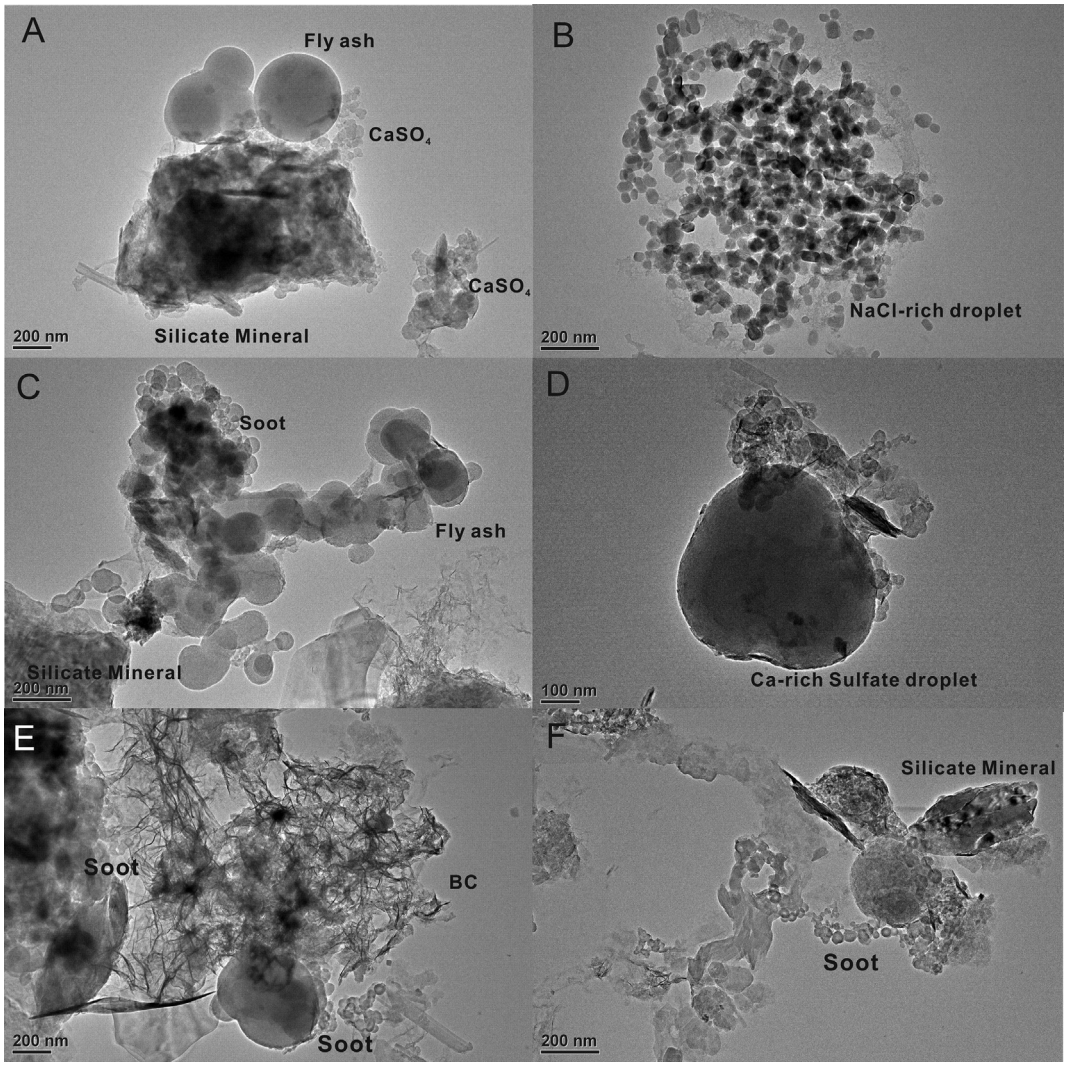

Fig. 4. Bright-field images of typical individual particles from the Ca-C grids: (a) a Silicate/Fly ash aggregate particle with additional mixed cation sulfate (MCS) components; (b) a NaCl-rich droplet; (c) a silicate/Soot/Fly ash aggregate particle; (d) a Ca-rich sulfate droplet; (e) a soot (ns)/mixed Black carbon aggregate particle; and (f) a silicate/soot aggregate particle.

BC concentration in the south (e.g., YL and ZD) could significantly change the albedo of snow and ice, at a greater rate than dust, which may cause significant melting of the glaciers.

3.2. Source of the cryoconite components deposition in Tibetan Plateau

Based on the TEM-EDX analysis, we obtained the physico-chemical composition of cryoconite on the glaciers of the Tibetan Plateau, which need to be further analyzed and to determine the sources and atmospheric transport route, combined with the regional atmospheric circulation and individual cryoconite particles. From the above discussion, we have defined the possible sources for cryoconite particles, including: (i) mineral dust from natural source, (ii) anthropogenic particles (e.g., BC, fly ash, and soot) from pollutants emissions, such as metal production and combustion of fossil fuels (Pacyna and Pacyna, 2001), and (iii) biological particles, together with other particles, such as NaCl and MCS particles from atmospheric deposition. The cryoconite deposition was obviously influenced by the regional atmospheric environment in a large geographic range surrounding the Tibetan Plateau. Therefore, we needed to determine the possible sources and transport route of these individual particles.

In this study, the sampling locations were distributed across a long range and large scale, and the atmospheric environment was different in each glacier area (Fig. 1). YL and ZD basins are located in the south of the Tibetan Plateau, with a high ratio BC and fly ash particles deposition in cryoconite (accounting for 38% and 22%, respectively, Fig. 5), which is much higher than the other sites. As the Tibetan Plateau is extremely high and remote, the population is small and human industrial activity is limited, and thus the regional anthropogenic emissions are extremely low. However, as the YL and ZD basins are located near southern Asia, we can infer that the high concentration of BC and fly ash particles in cryoconite was likely caused by pollutants transported from South Asia. While at the other sites in the north (e.g., LHG, TGL and TS), the cryoconite was composed primarily of mineral dust, and the concentration of BC and soot was obviously lower than that of the YL and ZD basin, although there were also many BC and fly ash found in LHG. NaCl and MCS salt particles and their aggregated particles were also extremely different between sites. TS and LHG exhibited a higher concentration of NaCl and MCS particles, which could relate to the

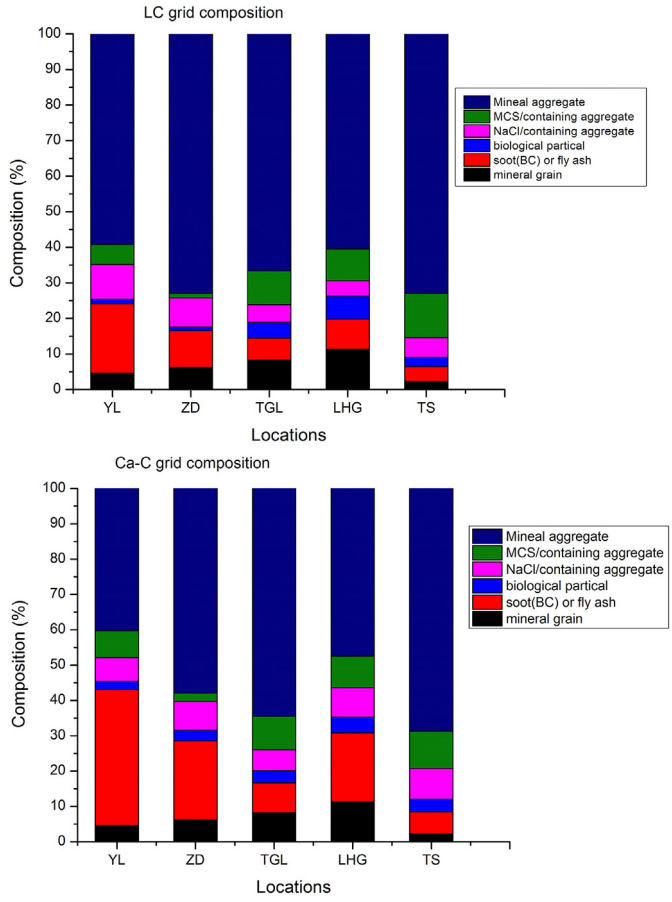

Fig. 5. The physical composition of the cryoconite on the glaciers in different areas of the Tibetan Plateau and the Tianshan Mountains in western China based on LC grid and Ca-C grid analysis.

regional emission of salt lake and anthropogenic emission in central Asia transported by the Westerlies.

The BC concentration in the LHG basin (northeastern Tibetan Plateau) was influenced by the regional industrial emissions, as LHG is near the Hexi Corridor in Gansu province with many large cities and many petroleum, iron and steel industries, which caused the higher ratio of BC in LHG cryoconite than TGL (the central Tibetan Plateau). In the TS glacier basin, the atmospheric environment was influenced primarily by large deserts in central Asia (e.g., Taklimakan and Gobi deserts), resulting in the higher concentrations of mineral dust in the cryoconite. Moreover, biological particles were also found with a large amount in TS.

The above inference also could be demonstrated from the regional atmospheric circulation and aerosol transport data. Fig. 6 shows the wind stream in the Tibetan Plateau and surrounding regions based on the NOAA/NCAR wind distribution and velocity data, showing the atmospheric circulation surrounding the Tibetan Plateau. Moreover, data from the Cloud Aerosol Lidar and Infrared Pathfinder Satellite Observation (CALIPSO) mission (http://www-calipso.larc.nasa.gov) were used to characterize the vertical distribution of the atmospheric pollution transportation around the Tibetan Plateau. Attenuated backscatter (reflectivity) profiles at 532 nm were provided by the Cloud-Aerosol Lidar with Orthogonal Polarization (CALIOP) installed on CALIPSO (Kutuzov et al., 2013; Winker et al., 2003) with vertical and horizontal resolutions of 60 m and 12 km, respectively. CALIOP/CALIPSO transact (Fig. 7) also clearly indicated the significant influence of atmospheric pollutant transportation from southern Asia to the southern Tibetan Plateau, and many pollutants were found also over the Qilian Mountains (LHG area). Combined with atmospheric circulation and CALIOP/CALIPSO transact, we determined that the southern location (YL and ZD) basins were impacted by the atmospheric pollutant from south Asia (both occurred in summer and winter) under the control of the Indian Summer Monsoon (ISM); while the northern locations (TGL and LHG) were influenced primarily by the Westerlies (particularly in the summer). Moreover, TS was impacted primarily

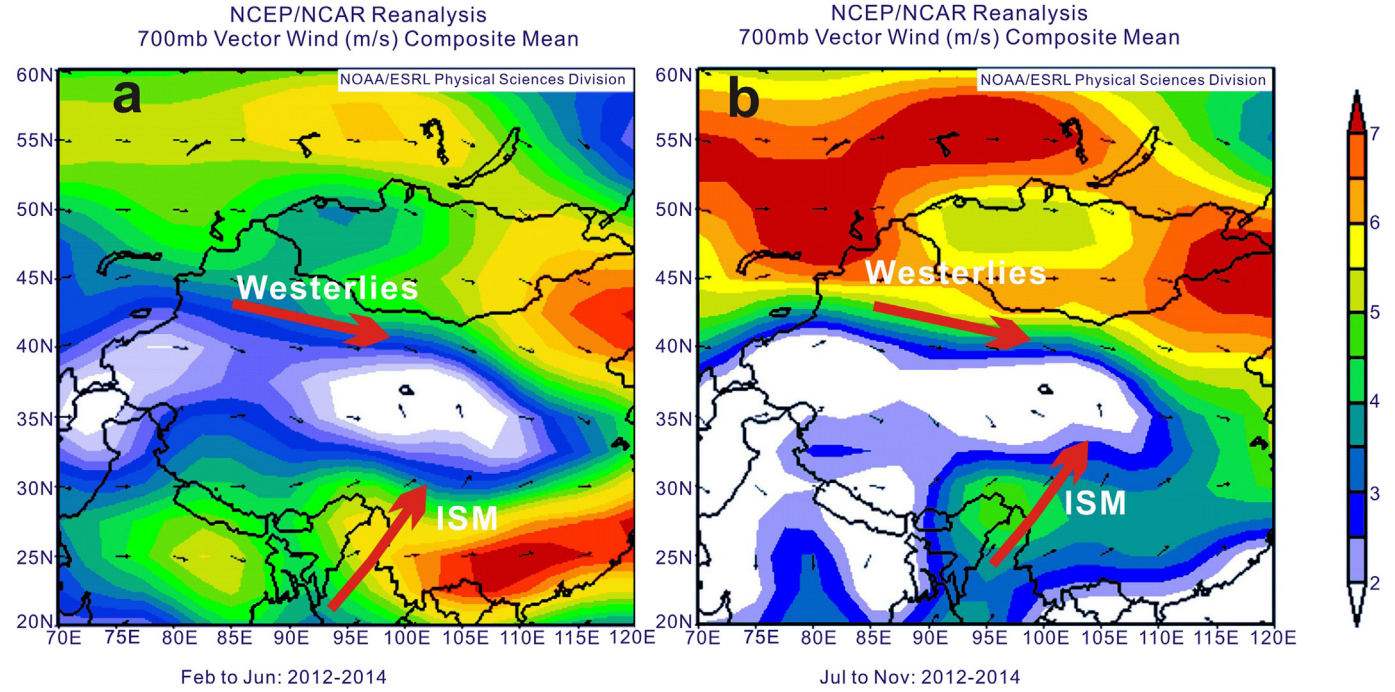

Fig. 6. The wind stream in the Tibetan Plateau and surrounding regions based on NCEP/NCAR reanalysis during 2012–2014 (a) winter and springtime, and (b) summer and autumn. ISM means Indian Summer Monsoon.

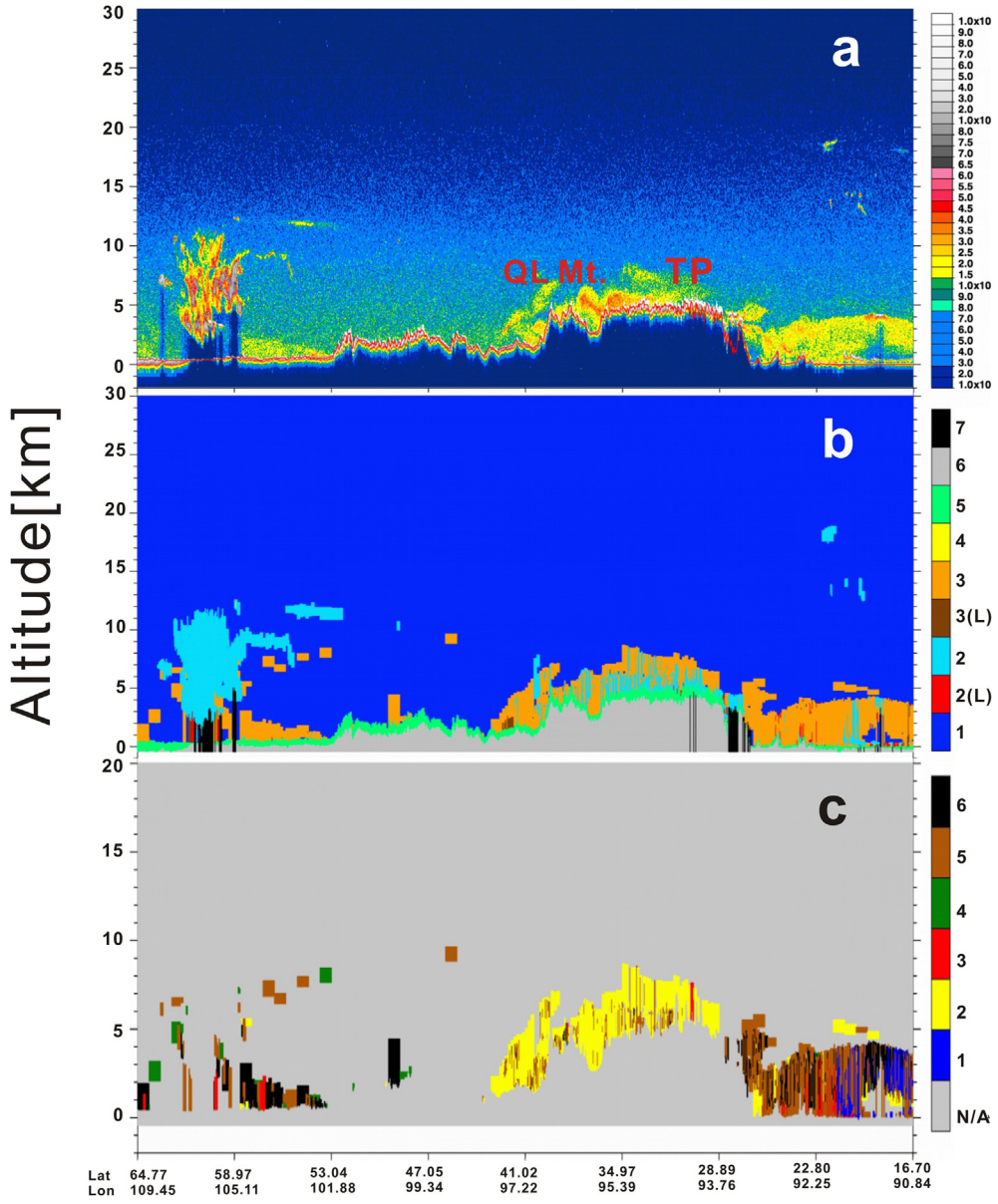

Fig. 7. **(a)** CALIOP vertical profile at 19:51 UTC on 25April 2014 showing the color-coded total attenuated back scatter Lidar return signal at 532 nm with green, yellow and red, indicating aerosols at low, medium and high concentrations, respectively. The TP in the figure indicates Tibetan Plateau, and The QL Mt. Means Qilian Mountains; **(b)**cloud-aerosol output, with 1 clear air, 2 cloud, 3 aerosol, 4 stratospheric layer, 5 surface, 6 subsurface and 7 totally attenuated; and**(c)**aerosol subtype profiles with 1 clean marine, 2 dust, 3 polluted continental,4 clean continental, 5 polluted dust and 6 smoke. (For interpretation of the references to colour in this figure legend, the reader is referred to the web version of this article.)

by the dust transport from arid deserts (Taklimakan deserts). These results also indicated that the deposition of light absorbing impurities in cryoconite was influenced primarily by the regional atmospheric environment and large-scale circulation.

Table 4 shows the TEM-EDX particle type and their chemical compositions of mineral dust particles in the cryoconite, using the

Table 4
The TEM-EDX particle type and the chemical composition of mineral dust particles in the cryoconite on the TGL Dongkemadi Glacier.

Type	Ratio (%)	Percentage of mass of various chemical elements (%)										
		Na	Mg	Al	Si	Cl	K	Ca	Ti	Fe	P	S
Si-rich	53.2	3.2	1.3	11.5	**57.1**	3.1	0.6	17.6	1.2	0.5	0.3	0.4
Ca-rich	18.5	2.6	6.2	6.5	9.8	4.1	5.4	**53.5**	2.5	0.8	3.5	2.1
Al-rich	12.9	8.8	2.5	**48.5**	13.5	10.1	0.4	8.0	0.5	5.5	–	0.8
Na-rich	5.5	**41.5**	8.3	8.5	2.4	20.5	0.8	2.3	4.3	6.5	–	–
Fe-rich	4.2	3.5	2.3	11	16.5	3.1	0.2	5.4	2.0	**38**	10.6	6.5

Bold numbers signifies the dominant element for mineral particles.

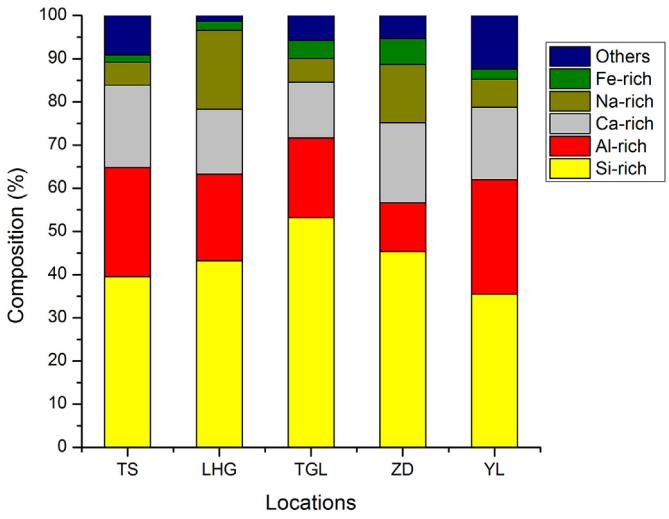

Fig. 8. TEM-EDX particle type and the chemical composition ratio (%) of mineral cryoconite on the glaciers of the Tibetan Plateau.

TGL Dongkemadi Glacier as an example, and Fig. 8 shows the TEM-EDX particle type and their chemical composition ratio of mineral cryoconite on the glaciers of the Tibetan Plateau. TEM-EDX revealed that the mineral particles in the cryoconite contained Si-, Al-, Ca-, Na-, and Fe-rich materials (Fig. 8), such as quartz, albite, and aluminate, This particle composition is similar to the chemical composition of Asian dust from the arid deserts in the central Asian region (Sun, 2005; Dong et al., 2014), which also could demonstrate the origin of regional mineral dust transport to the glacier cryoconite deposition on the Tibetan Plateau and TS glacier basins.

4. Conclusions

Cryoconite deposited on mountain glacier surfaces is significant for understanding regional atmospheric environments, which could influence the albedo and energy balance of glacier areas and maintain the glacial microbiology system. Field observations were conducted on the glaciers of western China, including LHG, TGL, ZD and YL, as well as TS for comparison with locations in the Tibetan Plateau, in addition to laboratory TEM-EDX analysis of the individual cryoconite particles filtered on LC and Ca-C TEM grids. This work provided information on the morphology and chemical composition, as well as a unique record of the particle's physical state, of cryoconite deposition on the Tibetan Plateau. The results revealed that cryoconite particle composition varied between different locations on the Tibetan plateau. In total, mineral dust particles were dominant (>50%) in the cryoconite at all locations. However, more anthropogenic particles (e.g., BC and fly ash), were found in YL (38%) and ZD (22%) in the southern locations. In TGL, many NaCl and MCS particles (>10%), as well as few BC and biological particles (<5%), were observed in cryoconite, in addition to mineral dust. In TS, the cryoconite was composed primarily of mineral dust with some BC (<5%). Compared with other sites, the LHG cryoconite exhibited a more complex composition of atmospheric deposition, with sufficient NaCl, BC, fly ash and biological particles (6% in the LC grid).

The higher ratio of anthropogenic particles in the southern Tibetan Plateau is likely caused by atmospheric pollutant transport from southern Asia to the Tibetan Plateau. Cryoconite in the northern locations (e.g., TGL, LHG and TS), containing higher dust and salt particle ratio, is influenced by the large deserts in central Asia. Therefore, the transport and deposition of cryoconite is significant for understanding the regional atmospheric environment and circulation. A large amount of biological, NaCl, and MCS particles were also found in the cryoconite, implying that, in addition to dust and BC, many types of light absorbing impurities combined could influence the glacier albedo change and induce ice melting in the mountain glaciers of the Tibetan Plateau. The TEM-EDX analysis showed that mineral particles in cryoconite contain primarily Si-, Al-, Ca-, Na- and Fe-rich materials, such as quartz, albite, and aluminate. This particle composition is similar to the composition of Asian dust from arid deserts in the central Asian region, which could also demonstrate the origin of regional mineral dust transport to the glacier cryoconite. A high BC concentration in the south (e.g., YL and ZD) could significantly change the albedo of snow and ice, at a greater rate than dust, which may cause significant melting of glaciers under global warming.

Acknowledgements

This work was funded by the National Natural Science Foundation of China (41301065, 41421061), the Chinese Academy of Sciences (KJZD-EW-G03-04), the State Key Laboratory of Cryospheric Sciences (SKLCS-ZZ-2016), the West Light Program for Talent Cultivation of Chinese Academy of Sciences, and the Youth Innovation Promotion Association, CAS (2015347). The authors would like to thank the field work team in summer of 2014 for their logistical work. We also gratefully acknowledge the NOAA/NCAR for the provision of the wind distribution and velocity data used in this publication, and acknowledge the data from the Cloud Aerosol Lidar and Infrared Pathfinder Satellite Observation (CALIPSO) mission. Moreover, anonymous referees are gratefully acknowledged for their constructive suggestions that help in improving the manuscript.

References

Anesio, A.M., Hodson, A.J., Fritz, A., et al., 2009. High microbial activity on glaciers: importance to the global carbon cycle. Glob. Change Biol. 15, 955–960.
Creamean, J.M., Suski, K.J., Rosenfeld, D., et al., 2013. Dust and biological aerosols from the Sahara and Asia influence precipitation in the western U.S. Science 339, 1572–1578. http://dx.doi.org/10.1126/science.1227279.
Dong, Z., Qin, D., Kang, S., Ren, J., et al., 2014. Physicochemical characteristics and sources of atmospheric dust deposition in snow packs on the glaciers of western Qilian Mountains, China. Tellus B 66, 20956. http://dx.doi.org/10.3402/tell us b.v66.20956.
Dong, Z., Kang, S., Qin, X., Li, X., Qin, D., Ren, J., 2015. New insights into trace elements deposition in the snow packs at remote alpine glaciers in the northern Tibetan Plateau, China. Sci. Total Environ. 529, 101–113.
Fujita, K., 2002. Impact of dust on glacier mass balance of the Tibetan Plateau. J. Arid. Land Stud. 11 (4), 355–360.
Grzesiak, J., Gorniak, D., Swiatecki, A., et al., 2015. Microbial community development on the 394 surface of hans and Werenskiold glaciers (svalbard, Arctic): a comparison. Extremmophiles 19 (5), 885–897.
Kutuzov, S., Shahgedanova, M., Mikhalenk, V., et al., 2013. High-resolution provenance of desert dust deposited on Mt. Elbrus, Caucasus in 2009–2012 using snow pit and firn core records. Cryosphere 7, 1481–1498.
Margesin, R., Zacke, G., Schinner, F., 2002. Characterization of heterotrophic microorganisms in alpine glacier cryoconite. Arct. Antarct. Alp. Res. 34, 88–93.
Naegeli, K., Damm, A., Huss, M., et al., 2015. Imaging spectroscopy to assess the composition of ice surface materials and their impact on glacier mass balance. Remote Sens. Environ. 168, 388–402.
Nagatsuka, N., Takeuchi, N., Nakano, T., et al., 2014. Geographical variations in Sr and Nd isotopic ratios of cryoconite on Asian glaciers. Environ. Res. Lett. 9, 045007. http://dx.doi.org/10.1088/1748-9326/9/4/045007.
Oerlemans, J., Giessen, R.H., van den Broeke, M.R., 2009. Retreating alpine glaciers: increased melt rates due to accumulation of dust (Vadret da. Morteratsch, Switzerland). J. Glaciol. 55, 729–736.
Pacyna, J.M., Pacyna, E.G., 2001. An assessment of global and regional emissions of trace metals to the atmosphere from anthropogenic sources worldwide. Environ. Rev. 9, 269–298.
Singh, P., Kapse, N., Arora, P., et al., 2015. Draft genome of Cryobacterium sp. MLB-32, an obligate psychrophile from glacier cryoconite holes of high Arctic. Mar. Genomics 21, 25–26.
Semeniuk, T.A., Bruintjes, R.T., Salazar, V., Breed, D.W., Jensen, T.L., Buseck, P.R., 2014. Individual aerosol particles in ambient and updraft conditions below convective

cloud bases in the Oman mountain region. J. Geophys. Res. Atmos. 119 http://dx.doi.org/10.1002/2013JD021165.
Sun, J.M., 2005. Nd and Sr isotopic variations in Chinese eolian deposits during the past8 Ma: implications for provenance change. Earth Planet. Sci. Lett. 240, 454–466.
Salavati-Niasari, M., 2005. Synthesis and characterization of host (Nanodimensional pores of Zeolite-Y)–guest [unsaturated 16-Membered octaaza–macrocycle manganese (II), cobalt (II), nickel (II), copper (II), and zinc (II) complexes]. Nanocomposite Mater. Chem. Lett. 34, 1444–1445.
Stibal, M., Sabacka, M., Zarsky, J., 2012. Biological processes on glacier and ice sheet surfaces. Nat. Geosci. 5 (11), 771–774.
Takeuchi, N., Li, Z., 2008. Characteristics of surface dust on Urumqi Glacier No. 1 in the tien shan mountains, China. Arct. Antarct. Alp. Res. 40, 744–750.
Takeuchi, N., Kohshima, S., Seko, K., et al., 2001. Structure, formation, and darkening process of Albedo-reducing material (cryoconite) on a Himalayan glacier: a granular algal mat growing on the glacier. Arct. Antarct. Alp. Res. 33 (2), 115–122.
Takeuchi, N., Kohshima, S., Segawa, T., 2003. Effect of cryoconite and snow algal communities on surface albedo on maritime glaciers in south. Alsk. Bull. Glaciol. Res. 20, 21–27.
Wientjes, I.G.M., Van de Wal, R.S.W., Reichart, G.J., Sluijs, A., Oerlemans, J., 2011. Dust from the dark region in the western ablation zone of the Greenland ice sheet. Cryosphere 5, 589–601.
Winker, D.M., Pelon, J.R., McCormick, M.P., 2003. The CALIPSO mission: spaceborne lidar for observation of aerosols and clouds. In: Proc. SPIE 4893, Lidar Remote Sensing for industry and Environment Monitoring III, 1, pp. 1–11.
Wharton, R.A., McKay, C.P., Simmons, G.M., et al., 1985. Cryoconite holes on glaciers. BioScience 35 (8), 499–503.
Zinatloo-Ajabshir, S., Salavati-Niasari, M., Hamadanian, M., 2015. Praseodymium oxide nanostructures: novel solvent-less preparation, characterization and investigation of their optical and photocatalytic properties. RSC Adv. 5, 33792–33800. http://dx.doi.org/10.1039/C5RA00817D.
Zinatloo-Ajabshir, S., Salavati-Niasari, M., 2016. Facile route to synthesize zirconium dioxide (ZrO2) nanostructures: structural, optical and photocatalytic studies. J. Mol. Liq. 216, 545–551.